SERBIAN JOURNAL OF ELECTRICAL ENGINEERING
Vol. 20, No. 3, October 2023, 315-332

UDC: 621.3.091.2:621.314.1 **DOI: https://doi.org/10.2298/SJEE2303315V**

A New High Step-Up Active Clamp DC-DC Converter with High Efficiency

Mahmood Vesali[1]

Abstract: In this paper, a new high step-up converter with a simple structure is presented. The auxiliary circuit of the proposed converter is in the form of active clamp, which provides soft switching condition under zero voltage for the main and auxiliary switches, hence the converter has high efficiency. Since the auxiliary switch added in the converter works as an active clamp and has a complementary command with the main switch, the proposed converter is not complicated in terms of the control circuit and does not need to design a new control circuit. This converter has a high voltage gain that provides a high output voltage with a lower duty cycle, so it is suitable for a new energy production system such as a solar system. The proposed converter has been fully analyzed and in order to prove the theoretical analysis, an experimental prototype has been implemented and tested at a power of 500 W, which in this power an efficiency of about 97.3% has been obtained.

Keywords: High step-up, Efficiency, DC-DC converter, Soft switching.

1 Introduction

Today DC-DC converters are widely used in the industry [1]. There are many applications of these converters in the industry, such as circuit power supply [2], solar systems [3 – 6], fuel cell systems [7 – 9], wind energy systems [10], etc. In the systems such as photovoltaic, the voltage level is low and needs to be increased to a higher level for conversion to the grid voltage for which a DC-DC converter is needed. The conventional boost converter can increase the voltage with high duty cycle, but in this converter, when the duty cycle is increased, the losses on the main inductor increases very much, and the efficiency decreases. Therefore, high step-up converters are introduced [11 – 15], which use techniques to increase the output voltage at lower duty cycle. In the isolated type of the step-up converter, the output voltage can be increased with high turns ratio in transformer [16, 17]. This method is good, but in the isolated type, due to transmitted magnetic power, the efficiency level is low, which in systems such as photovoltaic, where efficiency is very important, these types are not applicable.

[1]Department of Electrical Engineering, Naqshejahan Higher Education Institute, Isfahan, Iran
mahmoodvesali645@gmail.com

Of course, if isolation is needed, this type should be used, even though the level of the efficiency is low.

For reduction the size of the elements, especially the magnetic elements, the switching frequency should be increased in the converters. But in the basic converters, with the increase in frequency, the switching losses caused by overlapping of the voltage and current increases. For this reason, soft switching techniques are recommended [18]. In these techniques, the goal is to eliminate or reduce overlap of the voltage and current of the semiconductor elements, especially switches [19]. Also, by eliminating sudden jumps in the voltage and current, EMI noise is reduced [20]. For diodes used in the converters, the turn-off moments are important, because if the diode turns off suddenly, the reverse recovery of the diode imposes large losses on the converter [21]. Therefore, for converter diodes, it is important to create soft switching conditions as zero current switching (ZCS), so that the current slowly becomes zero and the diode turns off. Various soft switching methods such as resonant [22], phase shift [23], zero current switching [24 – 26], zero voltage switching (ZVS) [27 – 29] and zero voltage zero current switching (ZVZCS) [30] have been proposed for the switch (or switches) of the converters. These methods can provide the stated conditions for the moments of turning on, turning off, or both.

Recently many high step-up converters are proposed. In [31] a new high step-up ZVS converter is presented. In this converter, high voltage gain is achieved using coupled inductors and capacitors. Also, there is high efficiency due to zero voltage switching condition. Although high voltage gain is achieved in the converter and the converter has good efficiency, the proposed converter has a very large number of the elements. The proposed converter also has four switches, which complicates the structure of the converter in terms of the control circuit. The proposed converter in [32] has a simpler structure with high gain and efficiency. But this converter has a high number of diodes, which increases conduction losses and decreases efficiency. Also, the converter has two switches with special control, which requires the design of a new control circuit for the converter. The converter introduced in [33] is a single switch converter, that the structure of the converter in terms of the control circuit is no different from a basic single-switch converter. Additionally, with the introduced structure, high voltage gain and good efficiency have been achieved. But the proposed converter provides resonant soft switching condition, which imposes a high current stress on the switch. Although it is a single-switch converter, the overall structure of the converter is very complex with a large number of the elements. This results in the increase of the size and cost of the converter. In [34], a two-switch converter, with simple control on the switches is introduced. The switches are complementary to each other so there is no need to design a new control circuit. The proposed converter has a high gain, but this high gain is obtained by a complex structure that uses a large number of elements in the converter.

In this paper, a high step-up converter with a simple structure is presented. It uses only one coupled inductors and one capacitor to achieve high voltage gain. Also, by an active clamp circuit, soft switching condition is provided as ZVS. The coupled inductors in the proposed converter structure are in the form of tapped coupled inductors, which reduces the volume of the coupled inductors and converter. The leakage inductance energy caused by the coupled inductors is discharged in the auxiliary circuit and does not damage the main switch. The structure and analysis of this converter is presented in Section 2. In Section 3 design of the elements is presented, while the results of the testing of the experimental prototype of the proposed converter are provided in Section 4. In Section 5, a comparison between the proposed converter and other converters is made. Finally, in Section 6 conclusion of the paper is given.

2 Topology and Analysis

Fig. 1 shows the structure of the proposed converter. As can be seen, the converter has one coupled inductors, which winding as tapped coupled inductors. This coupled inductors is placed to increase voltage gain. Also, a capacitor is placed series with the coupled inductors to increase the output voltage. A clamp circuit with one auxiliary switch is placed for creating soft switching.

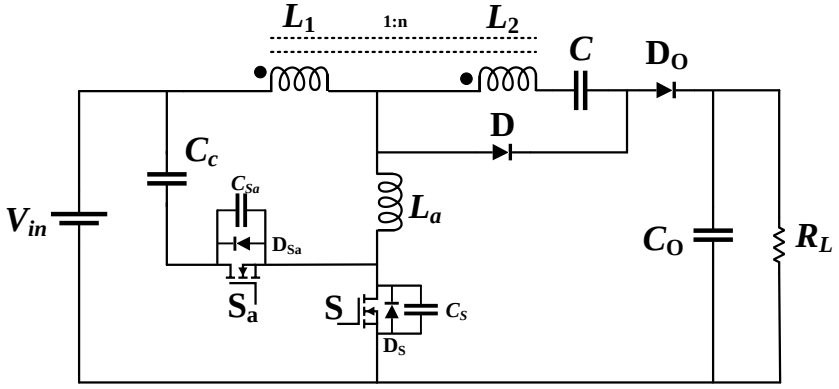

Fig. 1 – *The proposed converter structure*.

The proposed converter with the equivalent circuit of the coupled inductors, which consists of a magnetic inductor (L_m) and a leakage inductance (L_K), is shown in Fig. 2.

The converter has seven modes in one switching cycle. Before Mode 1 the main switch is off and the auxiliary switch is on. The key waveforms of the proposed converter are shown in Fig. 3.

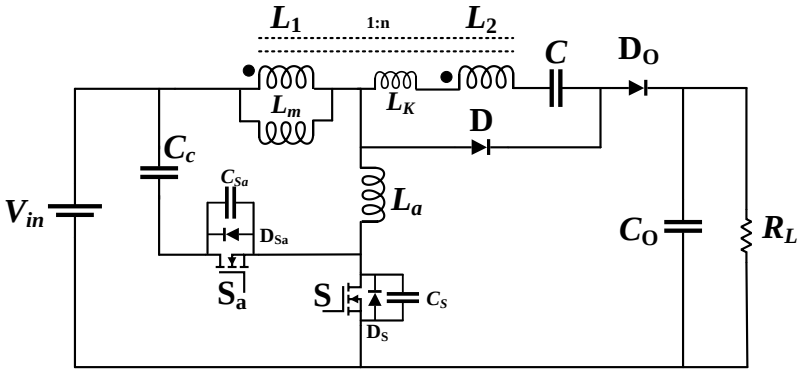

Fig. 2 – *The proposed converter with equivalent circuit of the coupled inductors.*

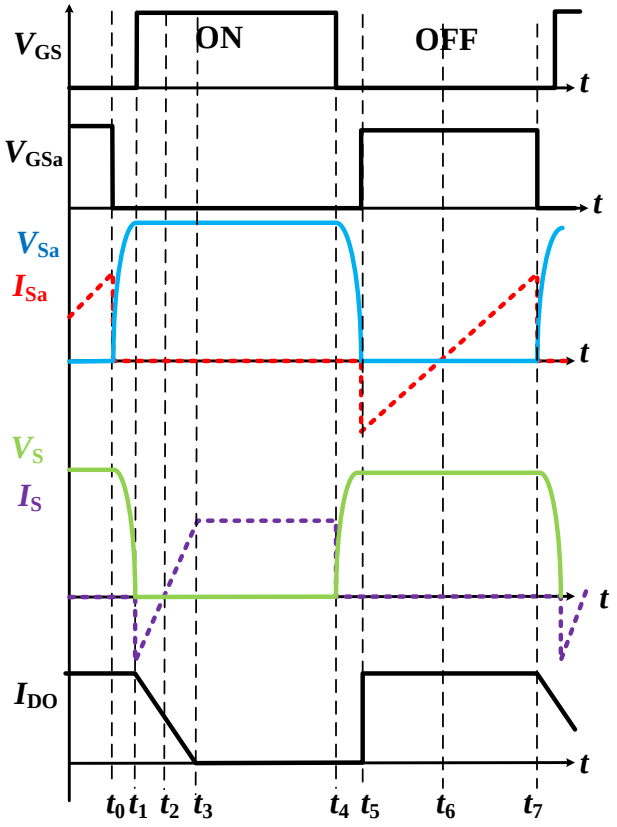

Fig. 3 – *The main waveforms of the proposed converter.*

Mode 1 ($t_0 - t_1$):

In the beginning of this mode, the auxiliary switch is turned off. Due to existence of L_a and current direction on this inductor, a resonance occurs between this inductor and snubber capacitors on the switches. This resonance causes the charging of C_{Sa} and discharging of C_S. Therefore, the voltage on the auxiliary switch increases slowly and ZVS condition is established for turning off distance. The equations of this mode are shown below:

$$V_{Csa} = V_{sa} = (V_{in} - V_{CC})\cos\omega_r (t - t_0) \tag{1}$$

$$I_{Csa} = \frac{(V_{in} - V_{CC})}{Z}\cos\omega_r (t - t_0) - I_{sa}(t_0) \tag{2}$$

$$Z = \sqrt{\frac{L_a}{C_{Sa}}} \tag{3}$$

$$\omega_r = \frac{1}{\sqrt{L_a (C_S + C_{Sa})}}. \tag{4}$$

Mode 2 ($t_1 - t_2$):

This mode starts when C_{Sa} is charged and C_S is discharged completely. Due to existence of body diode on the switch (S), when C_S voltage reaches to zero, this diode turns on and ZVS condition is established for S in turning on time. From this moment on, the switch is turned on under ZVS condition. In this mode, due to the placement of constant voltage on L_K, the current increases linearly until the current reaches zero. Also in this mode, the current of output diode (D_O) is decreased with same slope, so that ZCS condition is provided for this diode.

$$\alpha_1 = \frac{V_{in} - V_{Lm}}{L_a}, \tag{5}$$

where α_1 is slope of L_K current and switch current in this mode.

Mode 3 ($t_2 - t_3$):

The current of L_K reaches zero and the direction of this current is changed. So, the current is transmitted from the body diode to the switch, which is already turned on, and with the same slope as before continues to rise.

Mode 4 ($t_3 - t_4$):

In this mode, the switch current reaches I_{Lm}, and D_O turns off. Due to the current of the coupled inductors, D conducts and the current of the switch is fixed on I_{Lm}. This mode continues as long as the switch is on.

Mode 5 ($t_4 - t_5$):

When the main switch is turned off, this mode begins. Due to L_a, a resonance occurs between this inductor and snubber capacitors on the switches. C_{Sa} is discharged and C_S is charged. Therefore, the voltage on the main switch is increased slowly and ZVS condition is achieved. The equations for this mode are as follows:

$$V_{CS} = V_S = \left(V_{in} - V_{CC}\right)\cos\omega_r\left(t - t_0\right) \tag{6}$$

$$I_{CS} = \frac{V_{in} - V_{CC}}{Z}\cos\omega_r(t - t_0) - I_S(t_4) \tag{7}$$

$$Z = \sqrt{\frac{L_a}{C_S}} \tag{8}$$

$$\omega_r = \frac{1}{\sqrt{L_a\left(C_S + C_{Sa}\right)}}. \tag{9}$$

Mode 6 ($t_5 - t_6$):

When C_{Sa} is discharged completely, the body diode of S_a conducts and the voltage on this switch is clamped on zero. Therefore, ZVS condition is provided for this switch. The auxiliary switch is then turned on under ZVS condition. The switch current is increased linearly with slope given by (10). Also, in this mode, due to the current on auxiliary switch, D is turned off and D_O conducts.

$$\alpha_2 = \frac{V_{CC} - V_{Lm}}{L_a}, \tag{10}$$

where α_2 is current slope of the auxiliary switch in this mode.

Mode 7 ($t_6 - t_7$):

The current of L_a, as a resulting current of the auxiliary switch, reaches zero and the direction of it is changed. Therefore, the current is transferred from body diode to the switch and increases with α_2 slope. This mode ends when the auxiliary switch is turned off and the system turns back to Mode 1.

The equivalent circuits for the previously described modes are shown in Fig. 4.

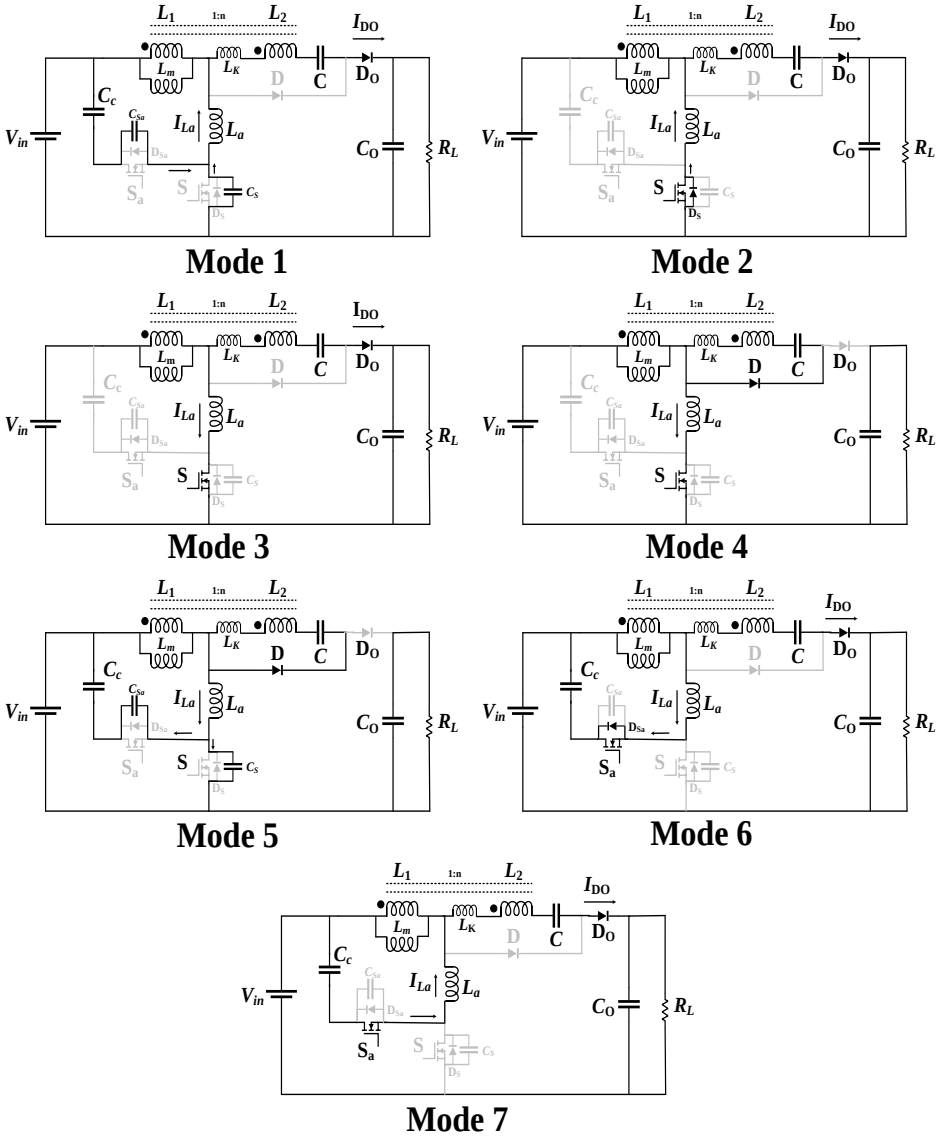

Fig. 4 – *The proposed converter equivalent circuits in seven modes.*

3 Elements Design

3.1 Main elements

The main elements of the converter such as L_m and C_O are chosen as for a boost converter. Therefore, L_m and C_O are obtained as below.

$$L_m = \frac{V_{in} D}{\Delta i_{Lm} f_{SW}} \tag{11}$$

$$C_{\mathrm{O}} = \frac{I_{\mathrm{O}}}{\Delta V_{\mathrm{CO}} f_{SW}}, \tag{12}$$

where Δi_{Lm} is variation of the main inductor current, which is usually considered to be 0.1 times the inductor current. Also ΔV_{CO} is variation of the output voltage that is considered 0.1 times of the output voltage. D is duty cycle of the main switch and f_{SW} is switching frequency.

The main switch (S) and main diode (D_O) of the converter are selected according to their voltage and current.

3.2 Auxiliary elements

The voltage gain is increased by adding L_2 and C. The value of these elements is obtained from voltage gain equation.

L_a establishes ZVS condition by fully discharging the snubber capacitors. So, the energy of this inductor should be sufficient.

$$\frac{1}{2} L_a I_{La}^2 > \frac{1}{2} C_{Seq} V_{CS}^2, \tag{13}$$

$$L_a > \frac{C_{Seq} V_{CS}^2}{I_{La}^2}, \quad C_{Seq} = C_S + C_{Sa}. \tag{14}$$

According to modes of the converter, V_{CS} is equal to $V_{in} - V_{CC}$ and I_{La} is equal to $I_{Lm}(1+1/n)$. Therefore, L_a is obtained as:

$$L_a > \frac{\left(C_S + C_{Sa}\right)\left(V_{in} - V_{CC}\right)^2}{\left(I_{Lm} + \frac{I_{Lm}}{n}\right)^2}. \tag{15}$$

As it is clear from (15), the snubber capacitors should be calculated first (16), (17) and then the inductance can be obtained.

$$C_S = \frac{i_{CS} t_f}{2 V_{CS}}, \tag{16}$$

$$C_{Sa} = \frac{i_{CSa} t_f}{2 V_{CSa}}, \tag{17}$$

where t_f is the switch current fall time specified for each switch by the manufacturer.

The noteworthy point is that the parasitic capacitance of each switch can also be used to create soft switching condition at the moment of turning on. However, due to the small value of these capacitance, when the switch is turned off, it is quickly charged and ZVS condition is not guaranteed.

As it is clear from the design relationships, many parameters effect the values of the elements, therefore, based on the design relationships and the desired range of the proposed converter, the curves in Figs. 5, 6 and 7 are found, which can help in the selection of the elements.

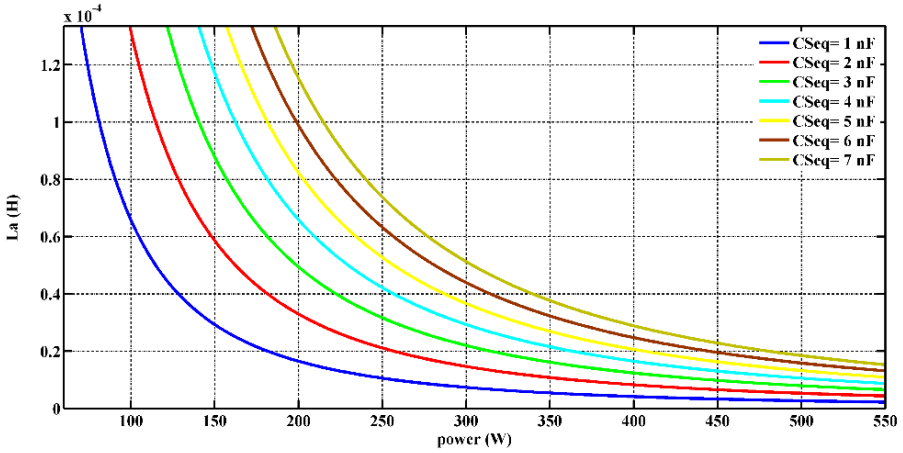

Fig. 5 – *The calculated values of L_a in respect to the power, for different values of C_{Seq}.*

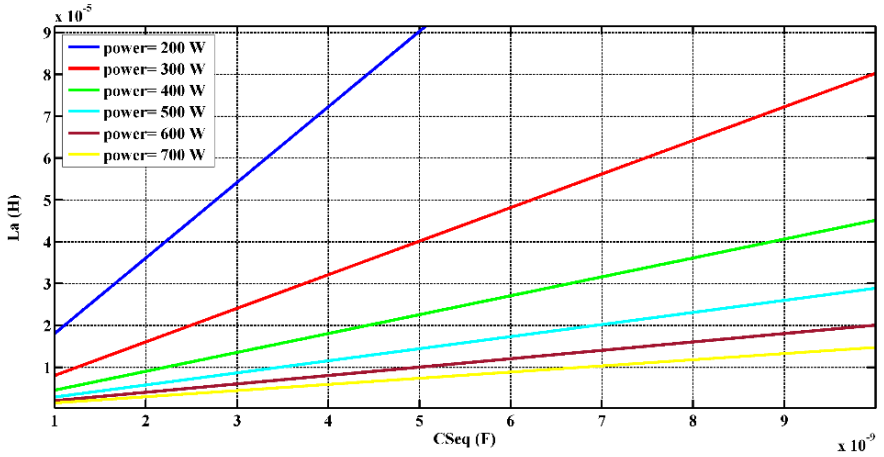

Fig. 6 – *The calculated values of L_a in respect to C_{Seq}, for different values of the power.*

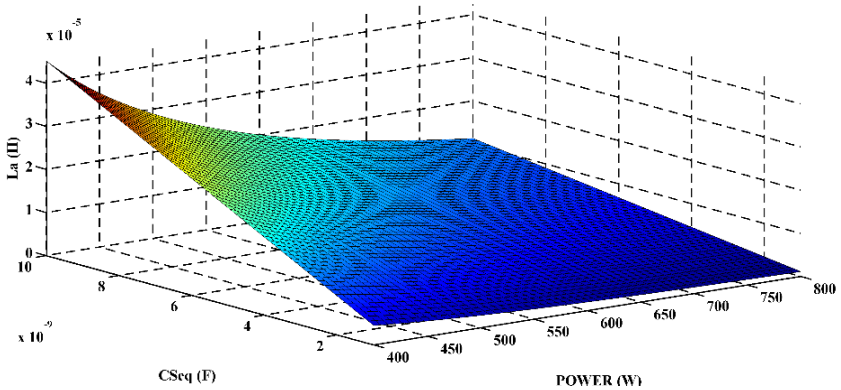

Fig. 7 – *The calculated values of L_a according to the power and C_{Seq}.*

3.3 Voltage gain

The voltage-second balance is written for L_m in order to obtain voltage gain:

$$V_{in}DT + \frac{V_{in} + V_C - V_O}{1+n}(1-D)T = 0\,. \tag{18}$$

It should be noted that some modes have been ignored due to their short working time.

In Mode 4, C is charged until $V_C = nV_{in}$. If this value is placed in (18), voltage gain is obtained as:

$$\frac{V_O}{V_{in}} = \frac{1+n}{1-D}\,. \tag{19}$$

The effect of n and D on the voltage gain are presented in Fig. 8. Curves are obtained according to (19).

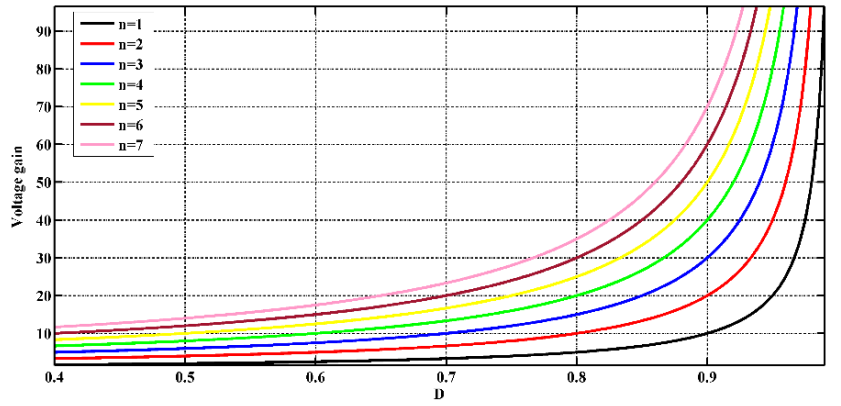

Fig. 8 – *The effect of D and n on voltage gain.*

4 Experimental Results

An experimental prototype of the proposed converter is shown in Fig. 9. It is made according to the specifications given in **Table 1**. Considering that the switching control is simple, the converter can be easily controlled by a ready controller. This controller is shown in Fig. 10. The experimental results of the prototype testing are presented in Fig. 11.

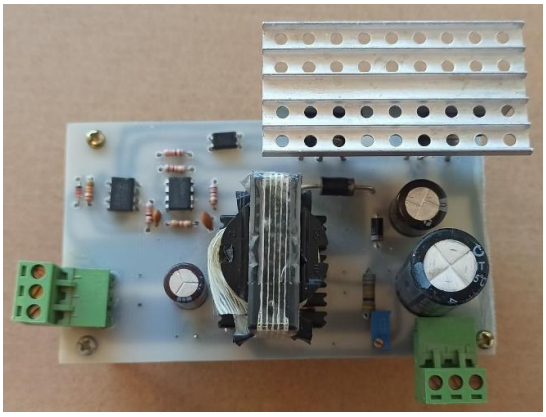

Fig. 9 – *The proposed converter.*

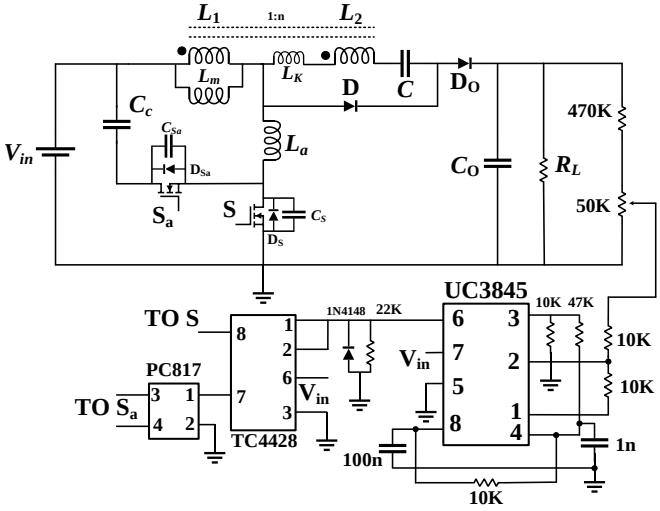

Fig. 10 – *The control circuit of the proposed converter.*

It can be noted from Fig. 11 that the current of the switches is negative when they are turned on, so, the ZVS condition is established. Also, the voltage is increased slowly, when the switches are turned off, which is how ZVS condition

is obtained. For diodes, the current slowly reaches zero when these diodes turn off, which explains how ZCS condition is established and reverse recovery problem does not exist.

Table 1
The proposed converter specifications.

ELEMENTS	PART NUMBER/ VALUE
D	MUR660
D_O	MUR260
S	IRFP140
S_a	IRFP140
L_m	400 µH
n	4
D	0.6
L_a	15 µH
C	10 µF
f_{SW}	100 kHz
C_O	100 µF
P	500 W

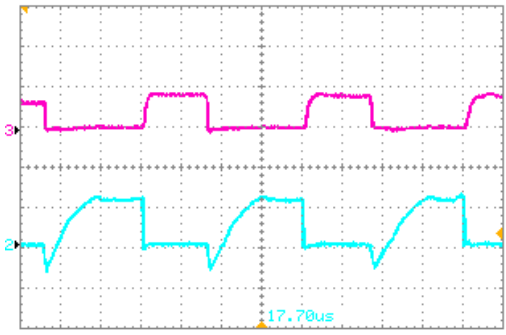

Fig. 11 – *Voltage* (*up*) *and current (down) of switch S* (*vertical scale is* 10 V/div *or* 20 A/div, *horizontal scale is* 2.5 µs/div).

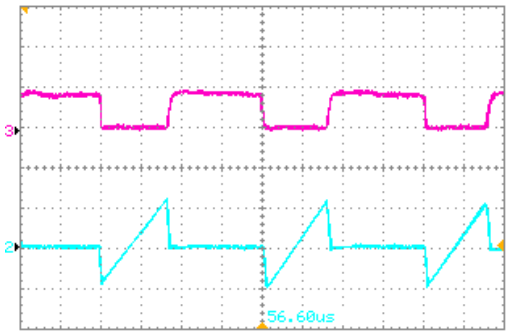

Fig. 12 – *Voltage* (*up*) *and current (down) of Sa* (*vertical scale is* 10 V/div *or* 20 A/div, *horizontal scale is* 2.5 µs/div).

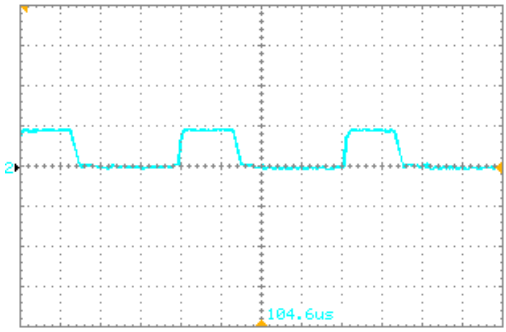

Fig. 13 – *Current of diode D* (*vertical scale is* 5 A/div, *horizontal scale is* 2.5 µs/div).

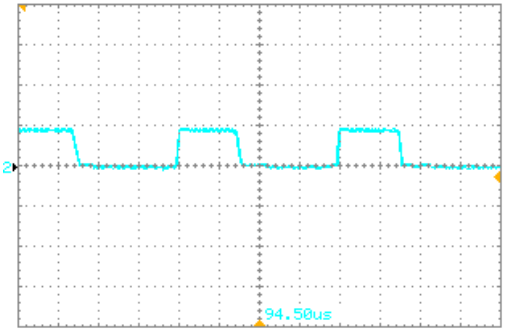

Fig. 14 – *Current of diode DO* (*vertical scale is* 2 A/div, *horizontal scale is* 2.5 µs/div).

5 Comparison Section

The proposed converter is compared with hard switching converter and in Fig. 12 the results are presented. As can be seen, the proposed converter has higher efficiency in comparison with hard switching converter.

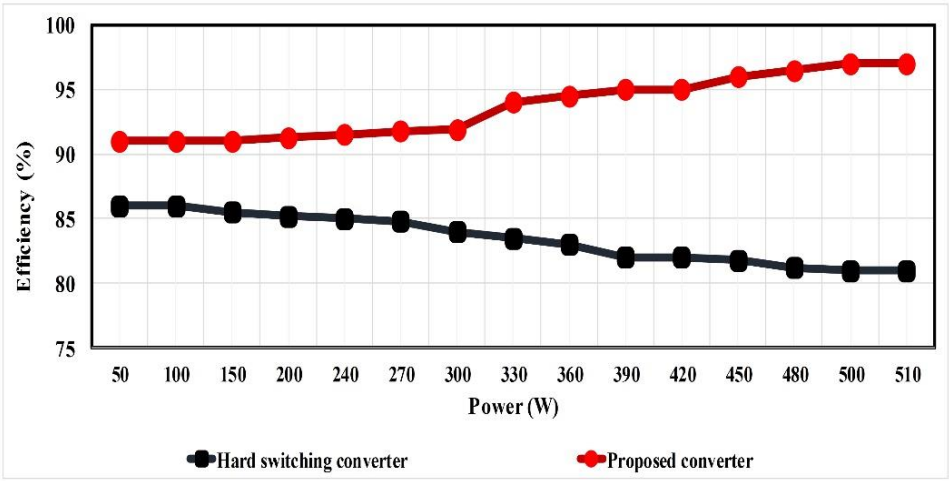

Fig. 15 –*The comparison of the efficiency of the proposed converter and hard switching type.*

Also, according to several important parameters, the proposed converter is compared with six converters that have been introduced in recent years (**Table 2**). The converters given in [31, 34] have high efficiency, and these converters have higher voltage gain than the proposed converter. However, this high gain has been obtained by a large number of the elements, which complicates the structure of the converters and increases the volume and cost. Converter proposed in [32] has good gain and good efficiency with small number of the elements. However, according to the proposed structure, this converter has a complex control over the switches, and for such a converter complex control circuit needs to be designed. Converter presented in [33] has a low efficiency with a large number of elements, although it has a very good and high voltage gain. Furthermore, converters given in [35, 36] have a small number of elements and their efficiency is also good, but both converters have a complex structure in terms of the control. Although, the converter proposed in this paper has a low gain compared to the other converters, it has a simpler structure both in terms of topology and control, while also having high efficiency.

Table 2
The comparison of the proposed converter with other soft switching converters.

Converter	Number of components	Soft switching for main switch	Efficiency	Voltage gain
[31]	24	ZVS	95.3 %	$\frac{n(m+1)+1}{n(m-1)(1-D)}$
[32]	13	ZVS	96.5 %	$\frac{2+n}{1-D}$
[33]	22	ZCS	94 %	$\frac{1+n_2+n_3+n_2(1+D)}{1-D}$
[34]	19	ZVS	97.52 %	$\frac{1+mN}{1-D}$
[35]	13	ZCS	95 %	$\frac{N(1+n)(1+D)+2}{1-D}$
[36]	14	ZCS	96.8 %	$\frac{1+n_{31}-n_{21}}{(n_{31}-n_{21})(1-D)}$
proposed	12	ZVS	97.3 %	$\frac{1+n}{1-D}$

6 Conclusion

A new DC-DC converter with high voltage gain was presented in this paper. The converter has simple structure with only one auxiliary switch. The auxiliary circuit worked as active clamp, which provided soft switching condition for the main and auxiliary switches. Therefore, the losses of the converter are reduced and the efficiency is increased. The auxiliary switch is switched complementary to the main switch, which did not complicate the control circuit, and the converter is also simple in terms of the control circuit. The aforementioned has been confirmed with theoretical analysis as well as the experimental results obtained for the prototype of the proposed converter.

7 References

[1] A. Nagarajan, S. J. Fusic: Analysis and Design of LCS Resonant Cell Based Enhanced Zero-Voltage Transition DC-DC Boosting Converter, Serbian Journal of Electrical Engineering, Vol. 16, No. 1, February 2019, pp. 105 – 121.

[2] M. Venkatesh Naik, P. Samuel: A High Efficiency Non-Inverting Multi Device Buck-Boost DC-DC Converter with Reduced Ripple Current and Wide Bandwidth for Fuel Cell Low Voltage Applications, Serbian Journal of Electrical Engineering, Vol. 15, No. 2, June 2018, pp. 165 – 186.

[3] S. Hasanzadeh, S. Mohsen Salehi, E. Najafi, F. Horri: High Voltage Gain Resonant DC-DC Converter with VM Cell for Renewable Sources Applications, Serbian Journal of Electrical Engineering, Vol. 19, No. 1, February 2022, pp. 1 – 14.

[4] N. R. Abjadi: Modeling and Realization of Photovoltaic Simulator Based on a Buck DC-DC Converter, Serbian Journal of Electrical Engineering, Vol. 19, No. 2, June 2022, pp. 147 – 166.

[5] A. Shoaei, K. Abaaszadeh, H. Allahyari: A Single-Inductor Multi-Input Multilevel High Step-Up DC–DC Converter Based on Switched-Diode-Capacitor Cells for PV Applications, IEEE Journal of Emerging and Selected Topics in Industrial Electronics, Vol. 4, No. 1, January 2023, pp. 18 – 27.

[6] R. Rahimi, S. Habibi, P. Shamsi, M. Ferdowsi: A Three-Winding Coupled-Inductor-Based Dual-Switch High Step-Up DC–DC Converter for Photovoltaic Systems, IEEE Journal of Emerging and Selected Topics in Industrial Electronics, Vol. 3, No. 4, October 2022, pp. 1106 – 1117.

[7] Z. Wang, Z. Zheng, C. Li: A High-Step-Up Low-Ripple and High-Efficiency DC-DC Converter for Fuel-Cell Vehicles, IEEE Transactions on Power Electronics, Vol. 37, No. 3, March 2022, pp. 3555 – 3569.

[8] L. Xu, R. Ma, R. Xie, S. Zhuo, Y. Huangfu, F. Gao: Offset-Free Model Predictive Control of Fuel Cell DC–DC Boost Converter with Low-Complexity and High-Robustness, IEEE Transactions on Industrial Electronics, Vol. 70, No. 6, June 2023, pp. 5784 – 5796.

[9] H. Bi, Z. Mu, Y. Chen: Common Grounded Wide Voltage-Gain Range DC–DC Converter with Zero Input Current Ripple and Reduced Voltage Stresses for Fuel Cell Vehicles, IEEE Transactions on Industrial Electronics, Vol. 70, No. 3, March 2023, pp. 2607 – 2616.

[10] G. F. Gontijo, T. Kerekes, D. Sera, M. Ricco, L. Mathe, R. Teodorescu: New Converter Solution with a Compact Modular Multilevel Structure Suitable for High-Power Medium-Voltage Wind Turbines, IEEE Transactions on Power Electronics, Vol. 38, No. 2, February 2023, pp. 2626 – 2645.

[11] P. Talebi, M. Packnezhad, H. Farzanehfard: Fully Soft-Switched Ultra-High Step-Up Converter with Very Low Switch Voltage Stress, IEEE Transactions on Power Electronics, Vol. 38, No. 3, March 2023, pp. 3523 – 3530.

[12] B.- X. Zhu, Y. Liu, S. Zhi, K. Wang, J. Liu: A Family of Bipolar High Step-Up Zeta–Buck–Boost Converter Based on "Coat Circuit", IEEE Transactions on Power Electronics, Vol. 38, No. 3, March 2023, pp. 3328 – 3339.

[13] L. Schmitz, D. C. Martins, R. F. Coelho: Three-Terminal Gain Cells Based on Coupled Inductor and Voltage Multipliers for High Step-Up Conversion, IEEE Transactions on Circuits and Systems II: Express Briefs, Vol. 70, No. 1, January 2023, pp. 236 – 240.

[14] A. Nikbahar, M. Monfared: A Family of High Step-Up Magnetically Coupled Impedance Source Inverters with Clamped DC-Link Voltage and Low Shoot-Through Current, IEEE Transactions on Power Electronics, Vol. 38, No. 1, January 2023, pp. 107 – 111.

[15] R. Heidari, E. Adib, K.- I. Jeong, J.- W. Ahn: Soft-Switched Boost–Cuk-Type High Step-Up Converter for Grid-Tied with Half-Bridge Inverter, IEEE Journal of Emerging and Selected Topics in Power Electronics, Vol. 11, No. 1, February 2023, pp. 786 – 795.

[16] K. Zaoskoufis, E. C. Tatakis: Isolated ZVS-ZCS DC–DC High Step-Up Converter with Low-Ripple Input Current, IEEE Journal of Emerging and Selected Topics in Industrial Electronics, Vol. 2, No. 4, October 2021, pp. 464 – 480.

[17] P. Jia, Z. Su, T. Shao, Y. Mei: An Isolated High Step-Up Converter Based on the Active Secondary-Side Quasi-Resonant Loops, IEEE Transactions on Power Electronics, Vol. 37, No. 1, January 2022, pp. 659 – 673.

[18] M. Vesali, M. Delshad, E. Adib, M. R. Amini: A New Nonisolated Soft Switched DC-DC Bidirectional Converter with High Conversion Ratio and Low Voltage Stress on the Switches, International Transactions on Electrical Energy Systems, Vol. 31, No. 1, January 2021, p. e12666.

[19] Q. Wang, Y. Wang, X. Liu, S. Zhang, G. Guo: A Soft-Switching High Gain DC–DC Converter for Renewable Energy Systems, International Journal of Electronics, Vol. 109, No. 4, April 2021, pp. 553 – 575.

[20] Z. Wang, H. Li, Z. Chu, C. Zhang, Z. Yang, T. Shao, Y. Hu: A Review of EMI Research in Modular Multilevel Converter for HVDC Applications, IEEE Transactions on Power Electronics, Vol. 37, No. 12, December 2022, pp. 14482 – 14498.

[21] H. Wen, J. Gong, X. Zhao, C.- S. Yeh, J.- S. Lai: Analysis of Diode Reverse Recovery Effect on ZVS Condition for GaN-Based LLC Resonant Converter, IEEE Transactions on Power Electronics, Vol. 34, No. 12, December 2019, pp. 11952 – 11963.

[22] Z. Zhang, X. Xiao, W. You, H. Li, T. Jin: A Novel Bidirectional Wider Range of Boost-Buck Three-Level LCC Resonant Converter as an Energy Link, IEEE Transactions on Power Electronics, Vol. 38, No. 2, February 2023, pp. 2143 – 2155.

[23] G. Liu, B. Wang, F. Liu, X. Wang, Y. Guan, W. Wang, Y. Wang, D. Xu: An Improved Zero-Voltage and Zero-Current- Switching Phase-Shift Full-Bridge PWM Converter with Low Output Current Ripple, IEEE Transactions on Power Electronics, Vol. 38, No. 3, March 2023, pp. 3419 – 3432.

[24] W. Xiong, M. Wang, G. Ning, M. Su: A Single-Stage ZCS Boost Module for MVDC Collection Converters, IEEE Journal of Emerging and Selected Topics in Power Electronics, Vol. 2, No. 4, 2023, pp. 701 – 711.

[25] S. Christian, R. A. Fantino, R. A. Gomez, Y. Zhao, J. C. Balda: High Power Density Interleaved ZCS 80-kW Boost Converter for Automotive Applications, IEEE Journal of Emerging and Selected Topics in Power Electronics, Vol. 11, No. 1, February 2023, pp. 744 – 753.

[26] H. Bahrami, H. Allahyari, E. Adib: A Self-Driven Synchronous Rectification ZCS PWM Two-Switch Forward Converter with Minimum Number of Components, IEEE Transactions on Industrial Electronics, Vol. 69, No. 12, December 2022, pp. 12842 – 12850.

[27] P. N. Truong, N. A. Dung, Y.- C. Liu, H.- J. Chiu: A Nonisolated High Step-Down DC–DC Converter with Low Voltage Stress and Zero Voltage Switching, IEEE Transactions on Power Electronics, Vol. 38, No. 3, March 2023, pp. 3500 – 3512.

[28] J. Zhang, D. Sha, K. Song: Single-Phase Single-Stage Bidirectional DAB AC–DC Converter with Extended ZVS Range and High Efficiency, IEEE Transactions on Power Electronics, Vol. 38, No. 3, March 2023, pp. 3803 – 3811.

[29] D. Wang, W. Yu, G. Mann, D. Meyer, E. Tarmoom, S. Chentz, X. Zhang, K. Speer: Isolated 3-Level DC–DC Converter with Complete ZVS Using Magnetizing Inductors, IEEE Transactions on Power Electronics, Vol. 38, No. 2, February 2023, pp. 1910 – 1923.

[30] G. Xu, J. Wang, G. Ning, W. Xiong, M. Su: A Dual-Transformer-Based Three-Level DC–DC Converter with Wide ZVZCS Switching Range, IEEE Transactions on Circuits and Systems II: Express Briefs, Vol. 70, No. 2, February 2023, pp. 670 – 674.

[31] D. Amani, R. Beiranvand, M. Zolghadri, F. Blaabjerg: A High Step-Up Interleaved Current-Fed Resonant Converter for High-Voltage Applications, IEEE Access, Vol. 10, October 2022, pp. 105387 – 105403.

[32] S. Shabani, M. Delshad, R. Sadeghi, H. H. Alhelou: A High Step-Up PWM Non-Isolated DC-DC Converter with Soft Switching Operation, IEEE Access, Vol. 10, April 2022, pp. 37761 – 37773.

[33] S. Abbasian, H. S. Gohari, M. Farsijani, K. Abbaszadeh, H. Hafezi, S. Filizadeh: Single-Switch Resonant Soft-Switching Ultra-High Gain DC-DC Converter with Continuous Input Current, IEEE Access, Vol. 10, March 2022, pp. 33482 – 33491.

[34] P. Mohseni, S. Rahimpour, M. Dezhbord, Md. Rabiul Islam, K. M. Muttaqi: An Optimal Structure for High Step-Up Nonisolated DC–DC Converters with Soft-Switching Capability and Zero Input Current Ripple, IEEE Transactions on Industrial Electronics, Vol. 69, No. 5, May 2022, pp. 4676 – 4686.

[35] T. Nouri, N. Vosoughi Kurdkandi, O. Husev: An Improved ZVS High Step-Up Converter Based on Coupled Inductor and Built-In Transformer, IEEE Transactions on Power Electronics, Vol. 36, No. 12, December 2021, pp. 13802 – 13816.

[36] S. Hasanpour, M. Forouzesh, Y. P. Siwakoti, F. Blaabjerg: A Novel Full Soft-Switching High-Gain DC/DC Converter Based on Three-Winding Coupled-Inductor, IEEE Transactions on Power Electronics, Vol. 36, No. 11, November 2021, pp. 12656 – 12669.